Reversal of temporal and spatial heterogeneities in tumor perfusion identifies the tumor vascular tone as a tunable variable to improve drug delivery

Philippe Martinive,[1] Julie De Wever,[1] Caroline Bouzin,[1] Christine Baudelet,[2] Pierre Sonveaux,[1] Vincent Grégoire,[3] Bernard Gallez,[2] and Olivier Feron[1]

[1]Unit of Pharmacology and Therapeutics, UCL Medical School; [2]Biomedical Magnetic Resonance Unit and Medicinal Chemistry and Radiopharmacy Unit; and [3]Center for Molecular Imaging and Experimental Radiotherapy, Brussels, Belgium

Abstract

Maturation of tumor vasculature involves the recruitment of pericytes that protect the endothelial tubes from a variety of stresses, including antiangiogenic drugs. Mural cells also provide mature tumor blood vessels with the ability to either relax or contract in response to substances present in the tumor microenvironment. The observed cyclic alterations in tumor blood flow and the associated deficit in chemotherapeutic drug delivery could in part arise from this vasomodulatory influence. To test this hypothesis, we focused on endothelin-1 (ET-1), which, besides its autocrine effects on tumor cell growth, is a powerful vasoconstrictor. We first document that an ET_A receptor antagonist induced relaxation of microdissected tumor arterioles and selectively and quantitatively increased tumor blood flow in experimental tumor models. We then combined dye staining of functional vessels, fluorescent microsphere-based mapping, and magnetic resonance imaging to identify heterogeneities in tumor blood flow and to examine the reversibility of such phenomena. Data from all these techniques concurred to show that administration of an ET_A receptor antagonist could reduce the extent of underperfused tumor areas, proving the key role of vessel tone variations in tumor blood flow heterogeneity. We also provide evidence that ET_A antagonist administration could, despite an increase in tumor interstitial fluid pressure, improve access of cyclophosphamide to the tumor compartment and significantly influence tumor growth. In conclusion, tumor endogenous ET-1 production participates largely in the temporal and spatial variations in tumor blood flow. ET_A antagonist administration may wipe out such heterogeneities, thus representing an adjuvant strategy that could improve the delivery of conventional chemotherapy to tumors. [Mol Cancer Ther 2006;5(6):1620–7]

Introduction

Tumor vasculature brings nutrients to the tumor but is also the main entry path for chemotherapy. Consequently, the use of antiangiogenic and antivascular drugs is complicated by the potential for reduced drug delivery as a result of vascular regression or destruction (1, 2). A detailed understanding of the tumor vascular compartment may lead to alternative strategies for improving therapeutic outcome (3). For example, if one considers the balance between immature and mature blood vessels in a given tumor, the response to antiangiogenic treatments may in part be anticipated. Indeed, it is now recognized that the presence of pericytes covering endothelial cells makes the mature vasculature less prone to apoptosis and thereby accounts for a form of resistance to antiangiogenic drugs (4–6).

In human cancers, tumor blood vessel maturation is likely to be an even more valid concept than in mice because the generally slower tumor growth offers more opportunities for pericytes to participate in microvessel structure. Eberhard et al. documented that microvessel pericyte coverage is consistently observed in malignant human tumors, reaching levels as high as 70% in mammary and colon carcinomas (7). Such reports on the thus far largely underestimated mature compartment of the tumor vasculature also shed new light on potential adjuvant treatments for conventional antitumor modalities. Indeed, the usual perception of a largely passive and unresponsive tumor vascular bed may be shifted to that of a vascular network, which may, at least locally and transiently, dilate or contract in response to alterations in the microenvironment or to exogenous stimuli.

This concept may be related to another paradigm called acute or intermittent hypoxia (8–10). Oxic-hypoxic cycles in tumors have been measured to occur with periodicities of minutes to hours (11, 12). Although this concept has now been clearly established by a variety of techniques, the

Received 11/14/05; revised 3/26/06; accepted 4/13/06.

Grant support: Fonds de la Recherche Scientifique, Fonds de la Recherche Scientifique Médicale, Fonds national de la Recherche Scientifique, Télévie, Belgian Federation Against Cancer, J. Maisin Foundation, and Action de Recherche Concertée grant ARC 04/09-317 from the Communauté Française de Belgique.

The costs of publication of this article were defrayed in part by the payment of page charges. This article must therefore be hereby marked advertisement in accordance with 18 U.S.C. Section 1734 solely to indicate this fact.

Note: O. Feron is a Fonds National de la Recherche Scientifique Senior Research Associate.

Requests for reprints: Olivier Feron, Unit of Pharmacology and Therapeutics (FATH 5349), UCL Medical School, 53 Ave E. Mounier, B-1200 Brussels, Belgium. Phone: 32-2-764-5349; Fax: 32-2-764-9322. E-mail: feron@mint.ucl.ac.be

doi:10.1158/1535-7163.MCT-05-0472

determinants of intermittent hypoxia are still poorly understood. The reason is probably that a combination of variables accounts for these temporal cycles, including fluctuations in hematocrit (9, 10, 13), local vascular remodeling due to angiogenesis (14), and alteration in the muscular tone of vessels (10). Nevertheless, as far as chemotherapy is concerned, it is mainly the latter source of variation that has to be considered. Indeed, whereas changes in red cell flux may only marginally influence drug access to the tumor, and angiogenesis alters the vasculature on a larger time scale, the variations in vasomotor tone are most likely to directly affect chemotherapeutic drug delivery. Importantly, this also suggests implicitly that adjuvant ''provascular'' treatments that adjust local tumor vascular tone have the potential to improve the efficacy of chemotherapy (3).

In this study, we combined (immuno)staining protocols and magnetic resonance imaging (MRI) to evaluate the integrity and the function of tumor blood vessels. We examined how the effects of endothelin-1 (ET-1), known to be up-regulated in many tumors (15) and to mediate not only cell proliferation but also vasoconstriction (16–19), could be counteracted by a specific (ET_A receptor) antagonist. Our data document that the tumor vasculature may benefit from such treatment, mostly through the correction of local/temporal ischemia within the tumor at the time of chemotherapy administration. These data emphasize that, in addition to the well-characterized structural defects in tumor vasculature, functional alterations in mature tumor blood vessels also constitute a source of heterogeneity in tumor blood flow but, importantly, seem to be reversible.

Materials and Methods

Mice, Tumors, and Treatments

NMRI, C57BL/6J, and C3H/He male mice (Elevage Janvier, Le Genest-St-Isle, France) were used in experiments with transplantable liver tumor (TLT; ref. 20), Lewis lung carcinoma (21), and fibrosarcoma-II (22) syngeneic tumor cells, respectively. Isoflurane-anesthetized mice received an i.m. injection of 10^5 to 10^6 tumor cells in the posterior right leg. The tumor diameters were tracked with an electronic calliper. When the tumor diameter reached 4.0 ± 0.5 mm, mice were randomly assigned to a treatment group. When indicated, they received an i.p. injection of the selective ET_A antagonist, BQ123 (Sigma, St. Louis, MO; 1 mg/kg) or saline alone. In some experiments, tumor-bearing mice were also injected i.p. with cyclophosphamide (25 or 100 mg/kg) or saline. Each procedure was approved by the local authorities according to national animal care regulations.

Myograph Assay

Tumor arterioles (100–300 μm) were dissected under a stereoscopic microscope and mounted on a 110P pressure myograph (DMT, Aarhus, Denmark), as previously detailed (23). Changes in the outer diameters were tracked and measured with the Myoview software (DMT). To establish the ET-1 dose-response curve, isolated arterioles were left to recover at physiologic pressure for 60 minutes in no-flow conditions in a physiologic salt solution medium (60 mm Hg, 37.5°C); additive doses of ET-1 (Sigma) were then delivered to the bathing medium. In some experiments, a 60-minute preincubation with BQ123 (1 μmol/L) was carried out. For each vessel used in this study, the ability of the vessels to contract upon application of a depolarizing KCl solution was verified at the end of the experiment and compared with a similar contraction done at the very beginning of the experiment. If these two contractions differed by 10%, the experiment was disregarded.

Tumor Blood Flow and Interstitial Fluid Pressure Monitoring

Tumor perfusion was measured with laser Doppler microprobes (Oxyflo; Oxford Optronics, Oxford, United Kingdom). Briefly, the probes were introduced into the tumor of isoflurane-anesthetized mice, and back scattering measurements were used to validate the absence of movement artifacts. Probes were also used to measure the perfusion in the thigh muscle of the contralateral leg (control). A 10-minute baseline of stable recordings was obtained before treatment administration through the catheterized tail vein; data were collected continuously at a sampling frequency of 20 Hz. In some experiments, laser Doppler imaging (Moor Instruments, Devon, United Kingdom) was also used to further validate the microprobe-derived data. Interstitial fluid pressure (IFP) was measured using the ''wick-in-needle'' technique, as previously described (24).

In situ Labeling of the Tumor Vascular Function and Structure

Fluorescent dye Hoechst 33342 (Sigma; 20 mg/kg) and 25-nm polymer microspheres (Duke Scientific Corp., Palo Alto, CA) were used to evaluate functional vasculature in the tumor. I.v. injection of microspheres was given 30 minutes after the i.p. administration of the ET_A antagonist BQ123 (1 mg/kg) or saline, and the tumors were excised from sacrificed animals 30 minutes later; the Hoechst 33342 dye was injected 1 minute before the sacrifice. Frozen samples of excised tumors were cryosliced and analyzed by fluorescence microscopy. Anti-CD31 antibodies (BD PharMingen, San Diego, CA) and adequate secondary antibodies coupled to TRITC or FITC fluorophores were used to costain endothelial cells on the same tumor slices.

Dynamic Contrast-Enhanced MRI

This technique was used to assess changes in tumor perfusion and tracer (P792) concentration in tumors before and after ET_A antagonist treatment, as described previously (11). Briefly, in isoflurane-anesthetized mice maintained in a fixed position, a first acquisition was done as control and a second one 30 minutes after i.p. injection of the ET_A antagonist BQ123 (1 mg/kg) or vehicle (saline). MRI was obtained with a 4.7-T (200 MHz, ^1H), 40-cm inner diameter bore system (Bruker Biospec, Ettlingen, Germany). For dynamic contrast-enhanced MRI (DCE-MRI) studies, two slices were selected: one was centered on the kidneys, and the second was positioned on the tumor. A set of 200 scans (512 seconds) was obtained in each acquisition sequence. After the first 12 images (used for baseline), the 6.5-kDa contrast agent P792 or Vistarem (Guerbet, France) was

delivered i.v. within 2 seconds (42 μmol/kg), and the signal intensity curve was sampled to track the fast increase in tissue signal enhancement. Before the second acquisition sequence, a set of 60 images was acquired over 1 hour to monitor the contrast agent washout. Contrast agent concentration as a function of time after P792 injection was estimated by comparing the signal intensities in the tumor and in a reference tissue (muscle) with known T1. The tracer concentration changes were fitted to a two-compartment pharmacokinetics model as previously described (11, 25, 26). Kinetics analyses were done as described previously (11, 24, 27). An operator-defined region of interest encompassing the tumor was analyzed on a voxel-by-voxel basis to obtain parametric maps. A power spectrum analysis was done to identify the number of voxels with statistically significant variations in signal intensity. To express the total amount of P792 in the tumor, the areas under the curve were calculated and compared for each experiment before and after ET_A antagonist or saline treatment.

Additional information on the DCE-MRI data analysis is provided as an Online Data Supplement.[4]

Terminal Deoxynucleotidyl Transferase–Mediated Nick-End Labeling Assay

Tumor cells cultured in 10% serum-containing DMEM were seeded into 16-well Labtek chamber slides. Confluent cells were deprived from serum and exposed to 0.25 μmol/L BQ123 (a dose that corresponds to an *in vivo* drug regimen leading to a theoretical 100% delivery to a 0.5-cm^3 tumor) and/or 4 μmol/L camptothecin (Sigma). Apoptotic cells were labeled by the terminal deoxynucleotidyl transferase–mediated nick-end labeling technique using a commercially available kit (Roche Diagnostics, Velvoorde, Belgium). Cell nuclei counterstained with 4′,6-diamidino-2-phenylindole were then examined with a Zeiss Axioskop microscope equipped for fluorescence.

Statistical Analyses

Data are reported as means ± SE; Student's *t* test and two-way ANOVA were used where appropriate.

Results

ET-1 Antagonist Induces Tumor Vessel Dilation *Ex vivo* and *In vivo*

To validate the possibility of reducing tumor vascular tone by using an endothelin antagonist in our experimental tumor models, we first aimed to verify *ex vivo* that isolated tumor arterioles could indeed respond to such a pharmacologic modulator. Tumor arterioles were microdissected from excised TLT tumors and mounted on a pressure myograph. After pressurization and equilibration, these vessels were exposed to increasing doses of ET-1, and the effect of a specific ET_A receptor antagonist BQ123 was evaluated. Figure 1A shows that low ET-1 concentrations caused vessel constriction, whereas BQ123-pretreated vessels did not respond. Of note, the ET_A antagonist already induced a ~15% vasodilation in the absence of any ET-1, reflecting the basal impregnation of tumor vessels by endogenously produced ET-1. To further confirm the high tumor selectivity of BQ123, we also administered the ET_A antagonist to mice bearing TLT and determined the effect on blood flow by using laser Doppler microprobes. Figure 1B shows that BQ123 (1 mg/kg) caused a net increase in tumor perfusion but did not alter the muscle perfusion in the contralateral leg. Similar results were found in two other tumor types (i.e., Lewis Lung carcinoma and fibrosarcoma-II), underscoring the ubiquitous nature of ET-1 overexpression and the associated (ET_A antagonist sensitive) increase in tumor vascular tone (see Fig. 1B). Of note, the lack of effect of the same dose of BQ123 on systemic blood pressure was confirmed in nonanesthetized mice using implanted telemetry devices (data not shown).

We next combined the CD31 immunostaining of tumor vascular structures with Hoechst 33342, which stains perfused vessels (at the time of i.v. injection). We found that the ET-1 antagonist increased the number of Hoechst 33342–labeled vascular structures considerably (79 ± 24% of CD31-positive structures per microscopic field versus 29 ± 14% in untreated tumors; $P < 0.01$; Fig. 1C). Of note, similar results were obtained when using antibodies directed against other endothelial markers (i.e., von Willebrand factor and MECA-32), thereby authenticating the endothelial nature of the CD31-labeled structures.

ET-1 Antagonist Increases Perfusion in Low-Flow Tumor Areas

We then used DCE-MRI to further examine tumor hemodynamics on exposure to the ET_A antagonist and, more particularly, to appreciate the occurrence of local intratumor differences. We first documented that the ET_A antagonist treatment increased the accumulation of the contrast agent in the whole tumor (versus control saline group; Fig. 2A). Quantitative analyses by area-under-the-curve measurements revealed that contrary to saline infusion, BQ123 administration consistently led to an increase in tumor perfusion whatever its basal level in a given tumor (i.e., the amounts of contrast agent in the considered tumor slice before BQ123 exposure; Fig. 2B). We also checked whether this increase corresponded to a homogeneous elevation of contrast agent concentration in the whole tumor or, as suspected, based on the data reported in Fig. 1C, whether local changes could be observed. Accordingly, voxel analyses revealed that in a 60-minute period, variations in contrast agent concentrations (i.e., the expected signal intensity pattern) occurred in approximately half of the tumor section, underscoring the basal heterogeneity in blood flow (Fig. 2C, *left*). Importantly, the frequency of the detected variations in contrast agent concentrations was consistently higher after ET_A antagonist infusion (see Fig. 2C and quantitative analyses in Fig. 2D).

ET-1 Antagonist Increases IFP and Decreases Convection Currents towards the Tumor

We then reasoned that the restoration of a homogenous perfusion within the tumor should alter IFP and influence the delivery of chemotherapeutics. Accordingly, we first

[4] Supplementary material for this article is available at Molecular Cancer Therapeutics Online (http://mct.aacrjournals.org/).

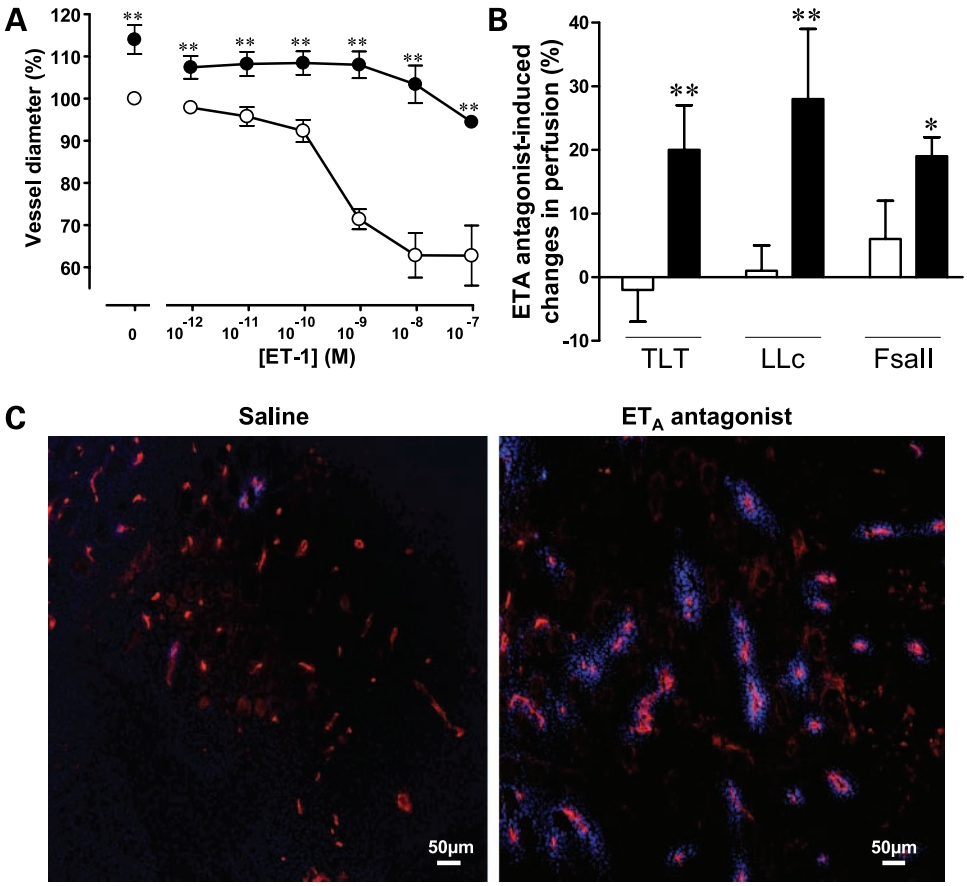

Figure 1. ET_A antagonist induces tumor arteriole relaxation *ex vivo* and reduces tumor blood flow heterogeneity *in vivo*. **A,** arterioles isolated from TLT-bearing mice were mounted on a pressure myograph and exposed to increasing doses of ET-1 in the presence (●) or absence (○) of the ET_A antagonist BQ123 (1 μmol/L). *Points,* mean percentages of the basal diameter obtained after vessel equilibration at 60 mm Hg internal pressure; *bars,* SE. Note the vasodilatory effects of the ET_A antagonist on the basal diameter (due to endogenous ET-1 impregnation). **, $P < 0.01$ ($n = 3-4$). For some conditions, SE are smaller than symbols. **B,** changes in perfusion determined 30 min after BQ123 injection by laser Doppler in the indicated tumor types (*black columns*) and the corresponding healthy thigh muscle of the contralateral leg (*open columns*). *, $P < 0.05$; **, $P < 0.01$ ($n = 3-6$). **C,** representative pictures of the effects of i.p. injection of saline or BQ123 (1 mg/kg) on the extent of TLT perfusion as determined by the comparison of Hoechst 33342 labeling (*blue*) and CD31-immunostained tumor vasculature (*red*).

aimed to verify the effect of the ET_A antagonist on IFP by the wick-in-needle technique. A net IFP increase (~100%) was observed both in small and large tumors upon ET_A antagonist treatment (Fig. 3A). In addition, to explore the effects of IFP increase, we looked for the extravasation of infused 25-nm fluorescent microspheres at the rim of the tumor where the IFP gradient is known to be steepest (i.e., rapidly increasing towards the tumor center). Figure 3B (*top*) shows that whereas large areas of bead extravasation were detectable in untreated tumors (saline), very few fluorescent beads could be found at the tumor/host tissue interface after ET_A antagonist treatment. Similar patterns were observed deeper in the tumor (see Fig. 3B, *bottom*). Interestingly, in untreated animals, analysis of the whole tumor sections revealed that microspheres accumulated in a heterogeneous manner, indicating the presence of clusters of differently perfused vessels at the time of bead injection. Colocalization of fluorescent beads and CD31-labeled vascular structures was even detectable in some areas, possibly reflecting beads trapped in (constricted) tumor vessels.

ET-1 Antagonist Improves the Delivery and the Therapeutic Efficacy of Cyclophosphamide

As a first insight into the effects of ET_A administration on the delivery of small therapeutic molecules (versus larger molecules as mimicked by microspheres), we first examined the fate of P792, the tracer that we used for DCE-MRI. With a molecular weight of 6.5 kDa, this compound is below the theoretical cutoff size (~10 kDa) of drugs that penetrate the tumor through convection currents from the vascular compartment. Pharmacokinetic analyses of the P792 concentration changes revealed that ET_A antagonist administration induced an increase in extravascular volume (V_e; Fig. 4A), strongly suggesting that, despite the simultaneous increase in IFP, molecules of a size similar to or smaller than P792 could benefit from the associated vasomodulatory treatment. To evaluate this potential adjuvant therapeutic effect of the ET_A antagonist, we examined the antitumor effects of cyclophosphamide, taken alone or in combination with BQ123. First, we used a low-dose (i.e., nontherapeutic) regimen of cyclophosphamide administration (25 mg/kg on days 0 and 1) and found that, when associated with the ET_A antagonist, a net growth delay was observed (see Fig. 4B). Indeed, whereas the doubling time for untreated tumors was similar to that of tumors treated with either treatment separately, the combined treatment increased the doubling time by 1.8-fold ($P < 0.01$, $n = 5-8$). In a second series of experiments, we used a higher dose of cyclophosphamide given at a 1-week interval (100 mg/kg on days 0 and 6). With this protocol, cyclophosphamide slowed down tumor growth but still did not prevent the doubling of the tumor

size in 2 weeks (see Fig. 4C). By contrast, coadministration of the ET_A antagonist with cyclophosphamide (100 mg/kg) limited tumor progression, with tumor size staying the same for 2 weeks with only two injections (Fig. 4C). Of note, the ET_A antagonist taken alone was inefficient (i.e., no difference in tumor growth versus untreated animals) at the dose used (1 mg/kg) but also at doses of 2 and 3 mg/kg (data not shown). Finally, to exclude a direct chemosensitizing effect of the ET_A antagonist, we also verified, on cultured TLT cells, that BQ123 did not increase the extent of apoptosis induced by serum deprivation or the apoptosis inducer drug camptothecin (Fig. 4D); note that the need for cyclophosphamide to be activated by the hepatic microsomal enzyme oxidation system prevented its use in this *in vitro* assay.

Discussion

The major findings of this study are that a large part of the topological heterogeneity in tumor perfusion is dependent on transient alterations in the tone of tumor vessels and, importantly, that pharmacologic correction of this defect is a reachable therapeutic objective. By combining different techniques, including dye staining of functional vessels, fluorescent microsphere-based mapping, and DCE-MRI, we have documented the existence of areas of nonuniform perfusion within tumors despite the presence of structurally defined blood vessels. We further identified ET-1, an abundant mitogenic molecule released by tumor cells, as a major trigger of these phenomena. This latter observation has important consequences because it offers a possible means of influencing a biological tumor variable that has thus far been difficult to manipulate and thereby acutely improving the delivery of chemotherapeutic drugs.

Tumor blood flow heterogeneity and resultant intermittent hypoxia have been documented in a large variety of tumors, including human cancers (13, 18, 28–32). Both spatial and temporal heterogeneities have been reported, and they usually relate to the opposition between

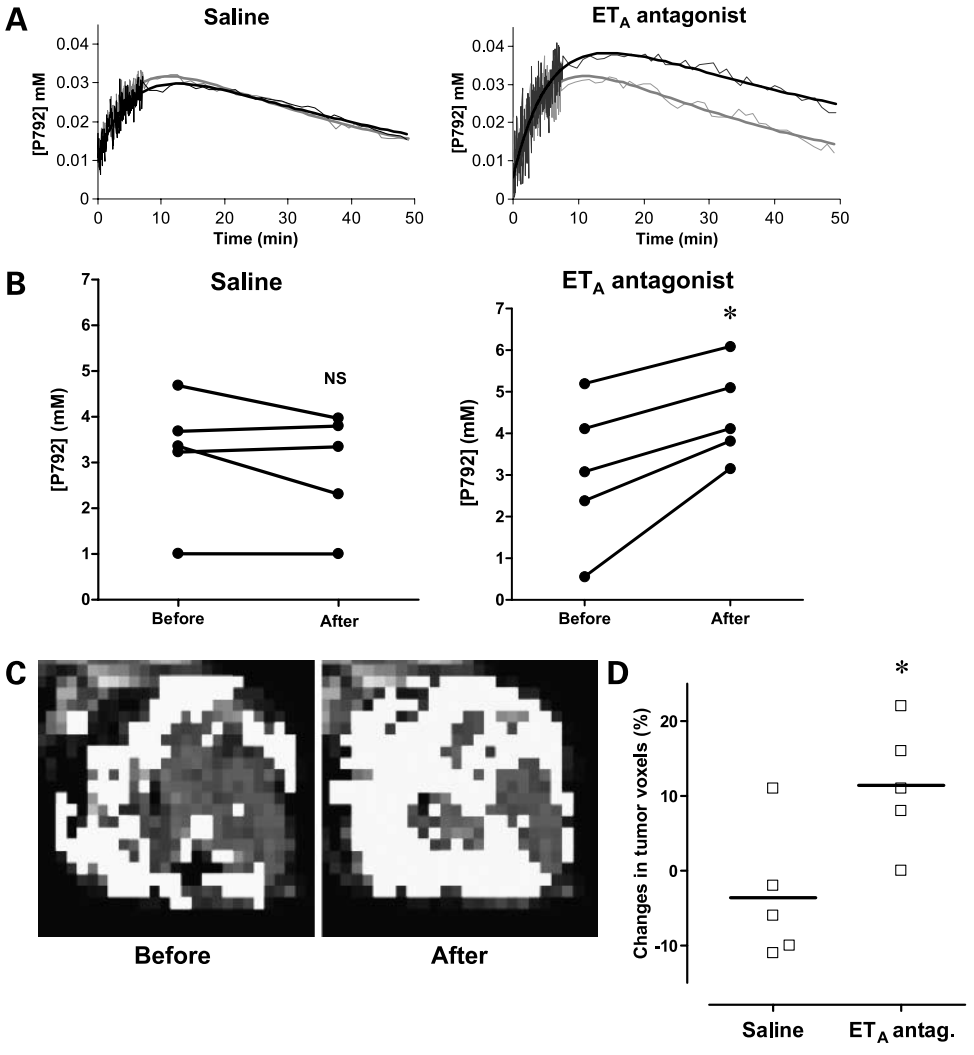

Figure 2. ET_A antagonist quantitatively and qualitatively increases tumor blood flow. DCE-MRI was used to compare the effects of BQ123 (1 mg/kg) or saline i.p. injection on TLT blood flow. **A,** representative curves depicting the time-dependent changes in the concentration of the contrast agent (P792) in tumors. Two acquisitions were done: one before (*gray*) and another 30 min after (*black*) injection of saline or ET_A antagonist. **B,** quantitative changes in contrast agent accumulation in different tumors before and after saline or ET_A antagonist injection. *, $P < 0.05$; NS = nonsignificant (paired test; $n = 5$). **C,** representative pictures mapping the tumor perfused voxels (*white*; i.e., tumor areas with significant variations in contrast agent concentrations during a 60-min period) before and after administration of the ET_A antagonist. **D,** quantitative changes in tumor perfused voxels induced by administration of saline or ET_A antagonist. *, $P < 0.05$ ($n = 5$).

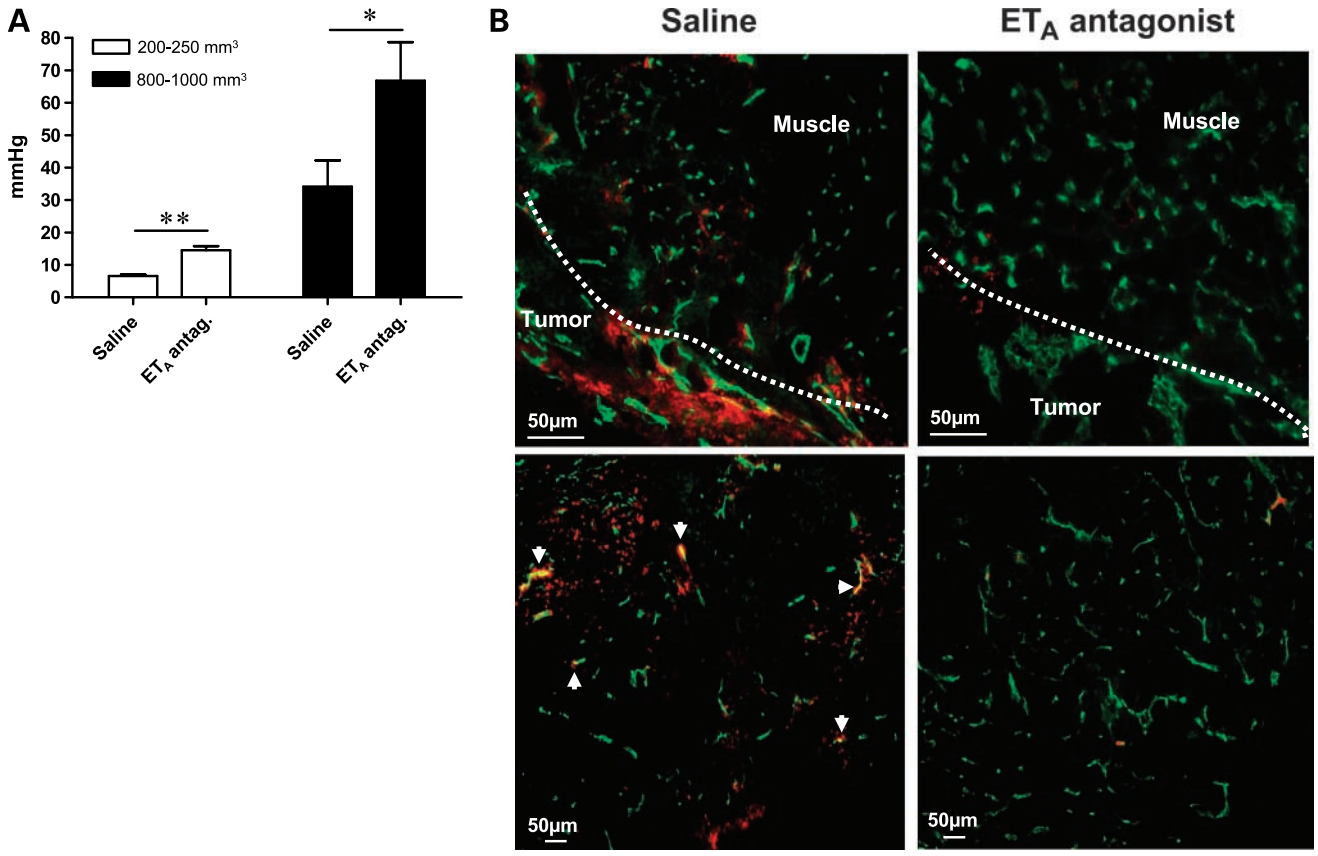

Figure 3. ET_A antagonist increases the tumor interstitial fluid pressure. **A,** changes in interstitial fluid pressure (as determined by the wick-in-needle technique) 30 min after administration of saline or the ET_A antagonist BQ123 (1 mg/kg) in small (*white columns*) and large (*black columns*) tumors. *, $P < 0.05$; **, $P < 0.01$ ($n = 6$). **B,** representative pictures of the accumulation of fluorescent microspheres (*red*) at the muscle-tumor interface (*top*) and in the center of the tumor (*bottom*) before and after administration of BQ123 (1 mg/kg). The tumor/muscle vasculature is costained with CD31 antibodies (*green*). Extravasation is reflected by the lack of superimposition of fluorescent microspheres with vascular structures, whereas costaining (*yellow*) is likely to correspond to the trapping of microspheres in (constricted) vessels (see *arrowheads*).

well-perfused areas at the tumor periphery and the poorly perfused center of the tumor and the intermittent stoppage of perfusion in some tumor areas. Although a variety of techniques has been developed to illustrate and validate these sources of tumor blood flow insufficiency and the associated hypoxic phenomena (9–12), the determinants of these phenomena are still poorly understood. Here, we provide new insights on the temporal component of tumor blood flow heterogeneity. Indeed, by showing the reversibility of the alterations in tumor microvascular flow by treatment with an ET_A antagonist (see Fig. 1C and Fig. 2C), we identified the alterations in the vascular tone of tumor vessels as an important cause of the intermittent changes in tumor blood flow.

We previously documented that ET_A antagonists could block the ET-1-mediated myogenic tone of tumor vessels, unraveling an important reserve of vasorelaxation within the tumor vasculature (19). This effect was further associated with a transient increase in tumor oxygenation and a higher efficacy of low-dose, clinically relevant fractionated radiotherapy (19). We now report that the same ET_A antagonist not only quantitatively but also qualitatively corrects a large part of the heterogeneity in tumor blood flow, promoting drug delivery and increasing the efficacy of conventional chemotherapy (see Fig. 4B and C).

The therapeutic potential of adjuvant treatments to increase permeability to drugs is a process dependent on the size of the chemotherapeutic molecule given but also on the tumor hemodynamics. Although not originally established to rationalize the diffusion and convection of drugs (<10 and >10 kDa, respectively) towards the tumor compartment, Fick's law and Starling's law enable the key determinants for drug delivery to be understood (33, 34). Accordingly, in both cases, the extent of drug transvascular delivery is directly proportional to the surface of exchange. The potential for ET_A antagonist-mediated vasodilation to affect drug delivery, therefore, relates certainly to this variable: any increase in the vessel radius leading to a 2π-fold more increase in vessel surface (if considering circular vessels). The size of the molecule will then determine whether an increase in the surface of exchange is positive or not for its delivery to the tumor compartment. Indeed, whereas for larger drug molecules (such as antibodies), the

hydrostatic force will determine whether the *convection* current is favorable; it is mainly the difference in concentration between the plasma and the tumor compartments that will govern the *diffusion* of small molecules (such as cyclophosphamide used in this study). Furthermore, the level of diffusion will be inversely related to the distance from the blood vessels. In our studies, both variables (i.e., drug concentration and distance) are very likely to be positively influenced by the administration of the ET_A antagonist. Indeed, local vasodilation increases the amount of drug present at a given time in the tumor, and, more importantly, decreasing the proportion of vessels with lower perfusion leads to a more homogeneous perfusion of the tumor, thereby increasing the chance for chemotherapy to reach a larger population of tumor cells.

A direct, sensitizing effect of ET_A antagonists coadministered with chemotherapy has been reported (15, 35). These effects are usually observed with ET_A antagonist regimens requiring daily administration for 2 to 3 weeks and leading to specific antitumor effects. These chemosensitizing effects are very unlikely to account for the tumor growth inhibition observed in our study considering the protocol of administration (two doses of ET_A antagonist on 1-day or at 1-week intervals; Fig. 4B and C) and the lack of apoptosis induction *in vitro* (see Fig. 4D). Conversely, the effect on tumor blood flow may have been underestimated in other studies examining the *in vivo* proapoptotic effects of chronic ET_A antagonist treatments. Future studies aiming to evaluate the therapeutic efficacy of the combination of ET_A antagonists with conventional chemotherapy will need to consider both the increase in drug delivery and the reduction in the threshold of resistance to apoptosis.

A net effect of the ET_A antagonist on IFP was observed in our experiments. This can be easily explained because arteriolar vasodilation increased microvascular pressure, which is thought to largely drive IFP (36). In fact, both components of the hydrostatic force are usually considered as nearly equal except at the tumor periphery where microvascular pressure > IFP. We verified this latter point in this study because the ET_A antagonist prevented the accumulation of microspheres at the rim of the tumor. The intimate relationship between microvascular pressure and IFP implies also that an increase in IFP does not lead to the collapse of tumor vessels. In addition, the tracer used in DCE-MRI has a molecular weight of 6.5 kDa and still extravasated significantly in the tumor compartment (see

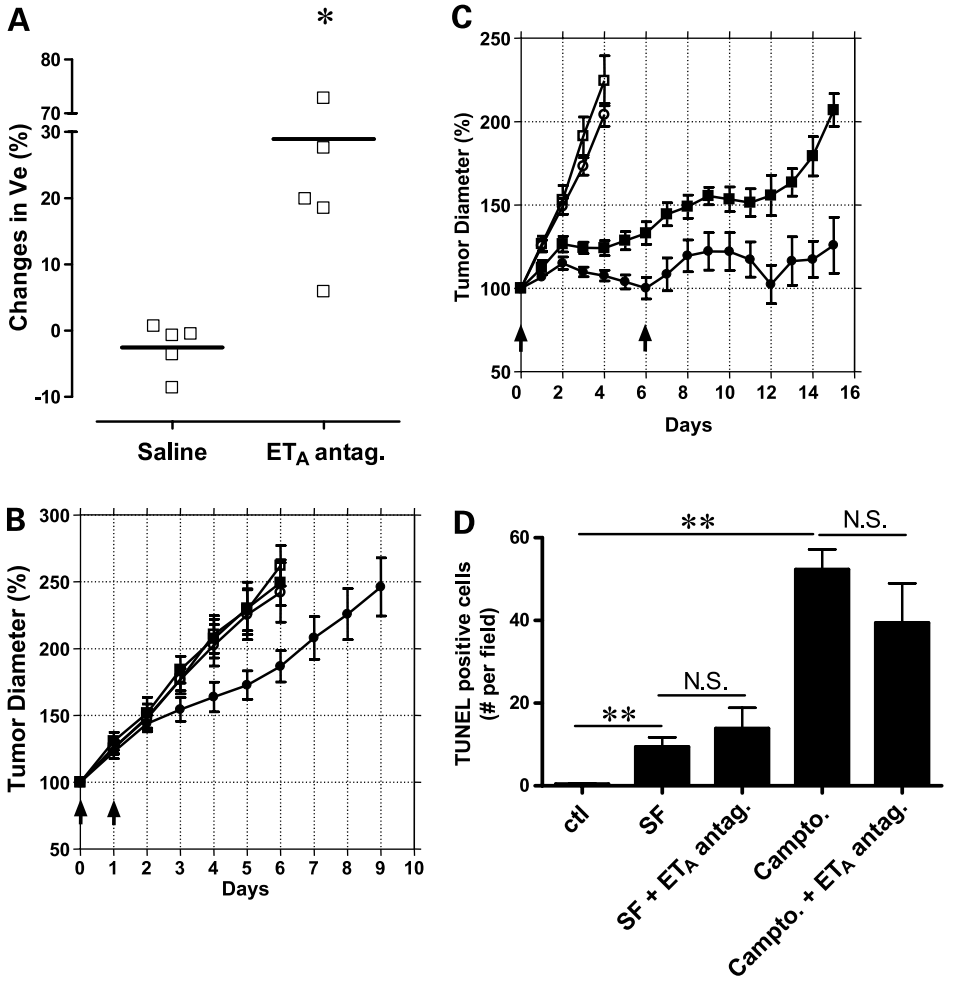

Figure 4. ET_A antagonist improves drug delivery to the tumor but does not exert antitumor effects per se. **A,** quantitative changes in the volume fraction of the extravascular, extracellular space (V_e) after administration of saline or the ET_A antagonist BQ123 (1 mg/kg), as determined by DCE-MRI using the contrast agent P792. *, $P < 0.05$ ($n = 5$). **B,** effect administration of the ET_A antagonist on drug delivery (and thereby therapeutic efficacy) was also evaluated by tumor growth measurements. Growth of TLT tumors was determined by measuring tumor diameters in control (saline-treated) mice (□) and in mice treated with 1 mg/kg BQ123 alone (○), with 25 mg/kg cyclophosphamide alone (■), and with the combination of cyclophosphamide and BQ123 (●). Cyclophosphamide and/or BQ123 were administered on days 0 and 1 (see *black arrows*); data are expressed as percentages of the initial tumor diameters ($n = 5-8$). **C,** same as in **B**, but a higher concentration of cyclophosphamide was used (100 mg/kg) and injections of cyclophosphamide and/or BQ123 were done on days 0 and 6. **D,** the extent of terminal deoxynucleotidyl transferase – mediated nick-end labeling – positive TLT cells (per microscopic field) in control (*ctl*) or serum-free (*SF*) conditions, in the presence (or not) of 0.25 μmol/L BQ123 and/or 4 μmol/L camptothecin. *Columns,* mean; *bars,* SE. *, $P < 0.01$; NS = nonsignifiant; $P > 0.05$ ($n = 3$).

Fig. 4A). Altogether, this indicates that the use of the ET_A antagonist should provide adjuvant effects for the delivery of most conventional chemotherapeutic drugs. For larger molecules, the data obtained with microspheres do not support such beneficial effects, but their diameter (around 25 nm) is still larger than macromolecules, and further experiments are needed to examine the effects of the ET_A antagonist on antibody delivery.

Finally, it is worth noting that the effects of the ET_A antagonist were very specific to the tumor vascular bed. The use of laser Doppler microprobes to measure perfusion in the healthy thigh muscle of the contralateral leg (see Fig. 1B) and telemetric devices to measure systemic blood pressure failed to reveal significant changes following ET_A antagonist administration. We have previously reported that the tumor selectivity of the ET_A antagonist was additionally supported by the higher density of ET_A receptors in tumor vessels (versus healthy vessels of the same diameter; 19). More generally, and in human cancers in particular, endothelin is increasingly recognized as a ubiquitous substance released in large amounts by many tumors (15). The large abundance of this cytokine in tumors probably accounts for the selectivity of the ET_A antagonist treatment. Several ET_A antagonists are currently engaged in different clinical trials to exploit their antitumor activities (15). The adjuvant properties identified in this study make the combination of ETA antagonist with other chemotherapeutic drugs even more relevant.

References

1. Kerbel R, Folkman J. Clinical translation of angiogenesis inhibitors. Nat Rev Cancer 2002;2:727 – 39.

2. Thorpe PE. Vascular targeting agents as cancer therapeutics. Clin Cancer Res 2004;10:415 – 27.

3. Feron O. Targeting the tumor vascular compartment to improve conventional cancer therapy. Trends Pharmacol Sci 2004;25:536 – 42.

4. McCarty MF, Liu W, Fan F, et al. Promises and pitfalls of anti-angiogenic therapy in clinical trials. Trends Mol Med 2003;9:53 – 8.

5. Benjamin LE, Golijanin D, Itin A, Pode D, Keshet E. Selective ablation of immature blood vessels in established human tumors follows vascular endothelial growth factor withdrawal. J Clin Invest 1999;103:159 – 65.

6. Gee MS, Procopio WN, Makonnen S, Feldman MD, Yeilding NM, Lee WM. Tumor vessel development and maturation impose limits on the effectiveness of anti-vascular therapy. Am J Pathol 2003;162:183 – 93.

7. Eberhard A, Kahlert S, Goede V, Hemmerlein B, Plate KH, Augustin HG. Heterogeneity of angiogenesis and blood vessel maturation in human tumors: implications for antiangiogenic tumor therapies. Cancer Res 2000; 60:1388 – 93.

8. Brown JM. Evidence for acutely hypoxic cells in mouse tumours, and a possible mechanism of reoxygenation. Br J Radiol 1979;52:650 – 6.

9. Kimura H, Braun RD, Ong ET, et al. Fluctuations in red cell flux in tumor microvessels can lead to transient hypoxia and reoxygenation in tumor parenchyma. Cancer Res 1996;56:5522 – 8.

10. Dewhirst MW, Kimura H, Rehmus SW, et al. Microvascular studies on the origins of perfusion-limited hypoxia. Br J Cancer Suppl 1996;27: S247 – 51.

11. Baudelet C, Ansiaux R, Jordan BF, Havaux X, Macq B, Gallez B. Physiological noise in murine solid tumours using T2*-weighted gradient-echo imaging: a marker of tumour acute hypoxia? Phys Med Biol 2004;49: 3389 – 411.

12. Dewhirst MW, Braun RD, Lanzen JL. Temporal changes in PO2 of R3230AC tumors in Fischer-344 rats. Int J Radiat Oncol Biol Phys 1998; 42:723 – 6.

13. Chaplin DJ, Hill SA. Temporal heterogeneity in microregional erythrocyte flux in experimental solid tumours. Br J Cancer 1995;71: 1210 – 3.

14. Patan S, Tanda S, Roberge S, Jones RC, Jain RK, Munn LL. Vascular morphogenesis and remodeling in a human tumor xenograft: blood vessel formation and growth after ovariectomy and tumor implantation. Circ Res 2001;89:732 – 9.

15. Nelson J, Bagnato A, Battistini B, Nisen P. The endothelin axis: emerging role in cancer. Nat Rev Cancer 2003;3:110 – 6.

16. Bell KM, Prise VE, Chaplin DJ, Wordsworth S, Tozer GM. Vascular response of tumour and normal tissues to endothelin-1 following antagonism of ET(A) and ET(B) receptors in anaesthetised rats. Int J Cancer 1997;73:283 – 9.

17. Bell KM, Chaplin DJ, Poole BA, Prise VE, Tozer GM. Modification of blood flow in the HSN tumour and normal tissues of the rat by the endothelin ET(B) receptor agonist, IRL 1620. Int J Cancer 1999;80: 295 – 302.

18. Chaplin DJ, Hill SA, Bell KM, Tozer GM. Modification of tumor blood flow: current status and future directions. Semin Radiat Oncol 1998;8: 151 – 63.

19. Sonveaux P, Dessy C, Martinive P, et al. Endothelin-1 is a critical mediator of myogenic tone in tumor arterioles: implications for cancer treatment. Cancer Res 2004;64:3209 – 14.

20. Taper HS, Woolley GW, Teller MN, Lardis MP. A new transplantable mouse liver tumor of spontaneous origin. Cancer Res 1966;26: 143 – 8.

21. Bertram JS, Janik P. Establishment of a cloned line of Lewis lung carcinoma cells adapted to cell culture. Cancer Lett 1980;11:63 – 73.

22. Volpe JP, Hunter N, Basic I, Milas L. Metastatic properties of murine sarcomas and carcinomas. I. Positive correlation with lung colonization and lack of correlation with s.c. tumor take. Clin Exp Metastasis 1985;3: 281 – 94.

23. Sonveaux P, Dessy C, Brouet A, et al. Modulation of the tumor vasculature functionality by ionizing radiation accounts for tumor radiosensitization and promotes gene delivery. FASEB J 2002;16: 1979 – 81.

24. Ansiaux R, Baudelet C, Jordan BF, et al. Thalidomide radiosensitizes tumors through early changes in the tumor microenvironment. Clin Cancer Res 2005;11:743 – 50.

25. Tofts PS. Modeling tracer kinetics in dynamic Gd-DTPA MR imaging. J Magn Reson Imaging 1997;7:91 – 101.

26. Su MY, Jao JC, Nalcioglu O. Measurement of vascular volume fraction and blood-tissue permeability constants with a pharmacokinetic model: studies in rat muscle tumors with dynamic Gd-DTPA enhanced MRI. Magn Reson Med 1994;32:714 – 24.

27. Baudelet C, Gallez B. Cluster analysis of BOLD fMRI time series in tumors to study the heterogeneity of hemodynamic response to treatment. Magn Reson Med 2003;49:985 – 90.

28. Chaplin DJ, Olive PL, Durand RE. Intermittent blood flow in a murine tumor: radiobiological effects. Cancer Res 1987;47:597 – 601.

29. Minchinton AI, Durand RE, Chaplin DJ. Intermittent blood flow in the KHT sarcoma-flow cytometry studies using Hoechst 33342. Br J Cancer 1990;62:195 – 200.

30. Pigott KH, Hill SA, Chaplin DJ, Saunders MI. Microregional fluctuations in perfusion within human tumours detected using laser Doppler flowmetry. Radiother Oncol 1996;40:45 – 50.

31. Durand RE, Aquino-Parsons C. Non-constant tumour blood flow-implications for therapy. Acta Oncol 2001;40:862 – 9.

32. Mollica F, Jain RK, Netti PA. A model for temporal heterogeneities of tumor blood flow. Microvasc Res 2003;65:56 – 60.

33. Yuan F, Dellian M, Fukumura D, et al. Vascular permeability in a human tumor xenograft: molecular size dependence and cutoff size. Cancer Res 1995;55:3752 – 6.

34. Netti PA, Hamberg LM, Babich JW, et al. Enhancement of fluid filtration across tumor vessels: implication for delivery of macromolecules. Proc Natl Acad Sci U S A 1999;96:3137 – 42.

35. Rosano L, Spinella F, Salani D, et al. Therapeutic targeting of the endothelin a receptor in human ovarian carcinoma. Cancer Res 2003;63: 2447 – 53.

36. Boucher Y, Jain RK. Microvascular pressure is the principal driving force for interstitial hypertension in solid tumors: implications for vascular collapse. Cancer Res 1992;52:5110 – 4.